Denial of bistatic hosting by spatial–temporal waveform design

H.D. Griffiths, M.C. Wicks, D. Weiner, R. Adve, P.A. Antonik and I. Fotinopoulos

Abstract: A set of theoretical techniques to prevent a radar from being used by a bistatic radar receiver as a non-cooperative illuminator are analysed. This works by radiating in addition to the radar signal waveform, a 'masking signal' waveform which is orthogonal to the radar signal waveform, both in the coding domain and the spatial domain. A number of different coding schemes are analysed. Two spatial coding methods are presented and analysed: the first uses a pair of interferometer elements at the extremities of the radar antenna array; the second uses a Butler matrix to generate a set of orthogonal beams. System-level calculations are presented to show the level of masking of the radar signal received by a bistatic radar receiver, and the suppression of the masking signal in the host radar echo. Some ideas for further work are presented.

1 Introduction

Many countries have invested heavily in the development of advanced surveillance systems and technologies. Of increasing concern is the threat that potential adversaries may use bistatic technologies to take advantage of significant investment in advanced sensors by our own countries [1, 2]. With relatively inexpensive receiver systems, an adversary could use the signals as bistatic 'illuminators of opportunity'. A central requirement for non-cooperative bistatic operation is the estimation of a coherent reference signal. This estimate is used to correlate with the received signals to extract the desired signal. As illustrated in Fig. 1, a coherent reference is typically obtained by measuring a direct path signal via the sidelobes of the illuminator [3, 4]. Conventional methods to prevent the interception of the direct path signal include low sidelobe antennas, physical isolation, and the use of spread-spectrum waveforms. These methods will become inadequate as surveillance sensors migrate to space.

This paper introduces and evaluates a number of theoretical techniques to prevent a radar being used by an adversary as a bistatic illuminator of opportunity. These are all based on the idea of radiating a so-called 'masking signal' (Fig. 2) which is arranged to be orthogonal, both in a spatial sense and in a coding sense, to the radar signal, and of a level sufficient to mask the radar signal to an adversary, and hence to deny a reference for bistatic operation [5, 6].

IEE Proceedings online no. 20041236

doi: 10.1049/ip-rsn:20041236

Paper first received 5th November 2001 and in revised form 22nd November 2004. Originally published online 4th March 2005

H.D. Griffiths is with University College London, Department of Electronic and Electrical Engineering, Torrington Place, London WC1E 7JE, UK

M.C. Wicks, D. Weiner and P.A. Antonik are with the Sensors Directorate, Air Force Research Laboratory, 26 Electronic Parkway, Rome, NY 13441-4514, USA

R. Adve is with the University of Toronto, Dept. of Electric and Communication Engineering, Communications Group, Rm. GB 434, 35 St. George St., Toronto, Ontario M5S 3G4, Canada

I. Fotinopoulos is with Imperial College of Science, Technology and Medicine, Department of Electrical and Electronic Engineering, Exhibition Road, London SW7 2BT, UK

E-mail: h.griffiths@ee.ucl.ac.uk

2 Waveform analysis and design

2.1 Ambiguity and cross-ambiguity functions

We consider a sideways-looking radar on an airborne platform, such as would be used for synthetic aperture radar (SAR) or ground moving-target indication (GMTI) purposes. As shown schematically in Fig. 2, the radar transmits (and receives) a radar waveform $u_r(t)$ at a power P_r via a radiation pattern $F_r(\theta)$, and transmits a masking waveform $u_m(t)$ at a power P_m via a radiation pattern $F_r(\theta)$. The waveforms may be pulsed, quasi-CW or CW. We wish to quantify the degree of masking of the radar signal at an adversary's bistatic receiver in a given direction, and the degree of suppression of echoes (from targets or from clutter) of the masking signal received in the channels of the radar receiver.

For a sideways-looking airborne radar and a stationary target, there is a direct relationship between echo Doppler shift f_D and angle θ such that

$$f_D = \frac{2v}{\lambda}\sin\,\theta \tag{1}$$

where v is the platform velocity and λ is the radar wavelength. Conventionally the performance of a radar waveform is quantified in terms of resolution, sidelobe structure, and ambiguities, in range and Doppler domains by means of the ambiguity function [7]. This plots the point target response of the radar as a function of delay (equivalent to range) and Doppler frequency (equivalent to velocity) by calculating the response of a matched filter for the waveform $u_r(t)$ to an echo of delay τ and Doppler shift f_D

$$\chi(\tau,f_D) = \int_{-\infty}^{\infty} u_r(t)u_r^*(t-\tau)e^{j2\pi f_D t}\,dt \tag{2}$$

The ambiguity function is defined as the square magnitude of this, $|\chi(\tau,f_D)|^2$. For our purposes, we are interested in the response of the radar receiver to an echo (from a target or from clutter) from the masking signal. This leads to the following definition of the cross-ambiguity function [8]:

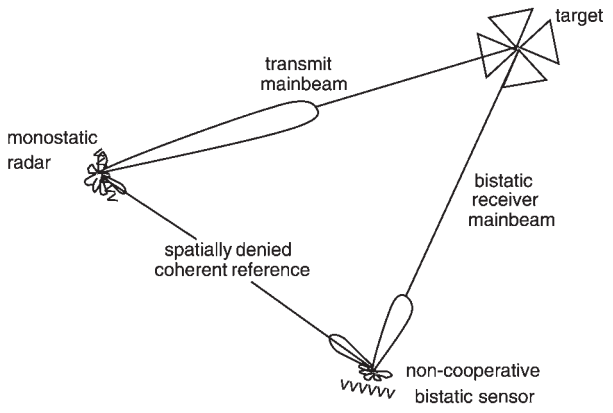

Fig. 1 *Non-co-operative bistatic receivers require coherent reference from host illuminator*

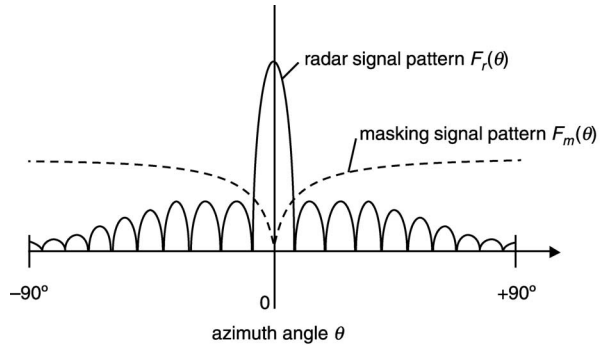

Fig. 2 *Radar and masking signal radiation patterns in which masking signal is radiated at level such that adversary cannot obtain reference from radar signal*

$$|\chi_{r,m}(\tau,f_D)|^2 = \left| \int_{-\infty}^{\infty} u_r(t) u_m^*(t-\tau) e^{j2\pi f_D t}\, dt \right|^2 \quad (3)$$

which is the response to a signal $u_m(t)$ (i.e. the masking signal) of a filter designed to be matched to waveform $u_r(t)$ (i.e. the radar signal).

2.2 Detection statistic of non-cooperative bistatic radar receivers

It is assumed that the non-cooperative bistatic radar receiver performs detection by utilising an estimate of the host radar transmitted signal for correlation with the received data. The estimate of the host radar transmitted complex envelope is typically obtained from the direct path signal observed by the bistatic radar receiver. In general, the direct path signal is corrupted by clutter and receiver noise which in some cases can be sufficient to cause significant signal processing losses due to poor estimates of the host radar complex envelope. However, for our purposes it is assumed that the masking signal is mainly responsible for degradation of the complex envelope estimate. In this way, there is no reliance solely on the clutter and receiver noise to prevent the non-cooperative bistatic radar receiver from 'hosting' off the monostatic radar. Of course, to the extent that the clutter and receiver noise help to mask the transmitted radar waveform in the direct path, the more difficult it will be for the non-cooperative bistatic radar receiver to operate successfully.

For simplicity assume that the direct path signal between the monostatic and bistatic radars is used as the coherent reference signal for the correlator in the non-cooperative bistatic radar receiver. Assume that the direct path signal intercepted by the bistatic radar receiver is delayed by an amount τ^{DP} and Doppler shifted by a frequency f^{DP}. If $n^{DP}(t)$ denotes the complex envelope of the receiver noise in the direct path the complex envelope of the direct path signal may be modelled as

$$u^{DP}(t) = K_{RAD}^{DP} u_r(t-\tau^{DP}) e^{j2\pi f^{DP}(t-\tau^{DP})} + K_{IFM}^{DP} u_m(t-\tau^{DP}) e^{j2\pi f^{DP}(t-\tau^{DP})} + n^{DP}(t) \quad (4)$$

where K_{RAD}^{DP} and K_{IFM}^{DP} are constants relative to the monostatic radar and masking signal powers intercepted by the bistatic radar, respectively.

The signal reflected from the target to the non-cooperative bistatic radar receiver consists of two components: one from the radar signal and one from the masking signal. Assume that the total path signal received by the bistatic radar receiver is delayed by an amount τ^{TP} and Doppler shifted by an amount f^{TP}. If $n^{TP}(t)$ denotes the complex envelope of the receiver noise in the total path the complex envelope of the total path signal may be modelled as

$$u^{TP}(t) = K_{RAD}^{TP} u_r(t-\tau^{TP}) e^{j2\pi f^{TP}(t-\tau^{TP})} + K_{IFM}^{TP} u_m(t-\tau^{TP}) e^{j2\pi f^{TP}(t-\tau^{TP})} + n^{TP}(t) \quad (5)$$

where K_{RAD}^{TP} and K_{IFM}^{TP} are constants relative to the target signal power intercepted by the bistatic radar due to the monostatic radar and the masking signal antenna, respectively. The bistatic delay is defined as $\tau_B = \tau^{TP} - \tau^{DP}$ and the bistatic Doppler shift is $f_B = f^{TP} - f^{DP}$. Ideally the non-cooperative bistatic receiver would like to correlate $u_r(t-\tau^{TP}) e^{j2\pi f^{TP}(t-\tau^{TP})}$ with the total path signal $u^{TP}(t)$. To accomplish this it would modify the direct path signal by a delay τ_B and a Doppler shift f_B. However, these are unknown in practice and so the bistatic radar receiver would utilise estimates of τ_B and f_B. Let these be denoted by $\hat{\tau}_B = \tau_B - \tau$ and $\hat{f}_B = f_B - \upsilon$. To detect a possible target the bistatic radar receiver would then correlate $u^{DP}(t-\hat{\tau}_B) e^{j2\pi \hat{f}_B (t-\tau^{DP}-\tau_B)}$ with $u^{TP}(t)$. This yields the test statistic employed for the detection of a target. Hence the test statistic at the output of the correlator in the non-cooperative bistatic radar receiver is

$$l = \int_{-\infty}^{\infty} [u^{DP}(t-\hat{\tau}_B)]^* e^{-j2\pi \hat{f}_B (t-\tau^{DP}-\hat{\tau}_B)} u^{TP}(t)\, dt \quad (6)$$

After some manipulation

$$l = e^{-j2\pi f^{TP}\tau} [k_1 \chi(\tau,\upsilon) + k_2 e^{j2\pi\upsilon\tau} Z^*(-\tau,-\upsilon) + k_3 Z(\tau,\upsilon) + k_4 \Gamma(\tau,\upsilon)] + \text{noise terms} \quad (7)$$

where $\chi(\tau,\upsilon)$ is the delay–Doppler ambiguity function of the host radar waveform, $Z(\tau,\upsilon)$ is the delay–Doppler cross ambiguity function between the interferometer and the host radar function, $\Gamma(\tau,\upsilon)$ is the delay–Doppler ambiguity function of the interferometer waveform, $k_1 = (K_{RAD}^{DP})^* K_{RAD}^{TP}$, $k_2 = (K_{RAD}^{DP})^* K_{IFM}^{TP}$, $k_3 = (K_{IFM}^{DP})^* K_{RAD}^{TP}$ and $k_4 = (K_{IFM}^{DP})^* K_{IFM}^{TP}$. The desired signal component of the detection statistic is $l_s = k_1 e^{-j2\pi f^{TP}\tau} \chi(\tau,\upsilon)$. The remaining terms represent noise and interference. In general, the desired signal component is corrupted by thermal noise, clutter, multipath and/or other propagation effects. However, it is the intention of this effort to design the masking signal such that it effectively masks the direct path signal from the host radar. The expression for the detection statistic clearly shows that the objective of coherent reference denial depends on the delay–Doppler ambiguity functions of the host radar and masking signal waveforms and their cross-ambiguity function.

2.3 Ambiguity functions of various signals

A simulation code has been devised to calculate and plot the auto- and cross-ambiguity functions of arbitrary signals, and to include the effect of antenna radiation patterns. In this Section we investigate the performance of various types of waveform; in the following Section we consider the effect of two different approaches to orthogonal radiation patterns.

2.3.1 Linear FM signals: An obvious candidate for the choice of radar and masking signals is to use two cochannel chirp waveforms of opposite slope. Waveforms of this type have been used by Giuli *et al.* in an application to simultaneously measure the elements of a polarimetric scattering matrix [9]. The auto-ambiguity function of a chirp signal has a rather high peak sidelobe level (PSL), around 13.2 dB, which can be lowered in the usual way by amplitude weighting. The cross-correlation of two opposite-slope chirp signals was evaluated for different values of time–bandwidth product BT. The results showed that for $BT = 1000$ the PSL was -33 dB and for $BT = 200$ it was -25 dB. The Doppler frequency shift was slightly smaller than the signal bandwidth, and the isolation loss due to Doppler shift was limited even when weighting was applied. Based on those results we conclude that the use of chirp signals for our purposes is limited because of range decorrelation between the compressed waveforms.

2.3.2 Pseudorandom binary sequences: Pseudorandom binary sequences (PRBSs) are another class of waveform with potentially useful properties in this context. Sets of PRBS codes of given lengths have been found with good auto- and cross-correlation properties [10]. To specify such codes we adopt the notation (n, m), where n denotes the decimal value of the shift register tap positions used to generate the code (the last tap is ignored because it is always used), and m is the decimal value of the binary number with which the shift register is loaded at the start of the code. The sequences used for this purpose are cyclic. For different sequences the first sidelobe levels had different values. For the sequence $(115, 115)$ of length 255 the PSL was -24.05 dB. For the sequence $(234, 413)$ of length 511 the PSL was found to be -27 dB. The Doppler tolerance is approximately $1/(\text{code length})$. The results showed that although the peak sidelobe levels are reasonable (of order 25 dB), the isolation between different codes is not so good. This problem is common in binary sequences and digital coding, where high isolation seems hard to achieve even if lower PSL values are accepted.

2.3.3 Costas signals: A third class of potentially useful waveforms are frequency-hopped waveforms [11, 12]. Frequency-hopped waveforms are conveniently represented by a square binary matrix known as the permutation matrix. An $N \times N$ matrix contains a total of $Q = N^2$ matrix elements. Thus, when the elements are binary, the number of different matrices possible is 2^Q. However, of these only $N!$ matrices can be obtained by permuting the N integers contained between 0 and $(N - 1)$. Some of these are better than others for designing the signal pattern of a radar waveform. Costas introduced a specific type of permutation matrices, the so-called Costas arrays [13, 14] which may be used in applications such as spread-spectrum communication systems, where the objective may be to achieve either jamming resistance, low probability of intercept, or frequency diversity for a selectively fading channel. An example of a Costas array for $N = 7$ is shown in Fig. 3, and the corresponding auto-ambiguity function in Fig. 4. The equivalent auto-ambiguity function for a Costas signal for which $N = 30$ is shown in Fig. 5. It can be seen in both cases that the ambiguity function, although it does not have a smooth pedestal, approaches the shape of the ideal 'thumbtack'.

$f_c + f_6$		*					
$f_c + f_5$				*			
$f_c + f_4$					*		
$f_c + f_3$	*						
$f_c + f_2$							*
$f_c + f_1$						*	
f_c			*				
f / t	t_0	t_1	t_2	t_3	t_4	t_5	t_6

Fig. 3 *Permutation matrix of one of 200 possible Costas arrays for $N = 7$*

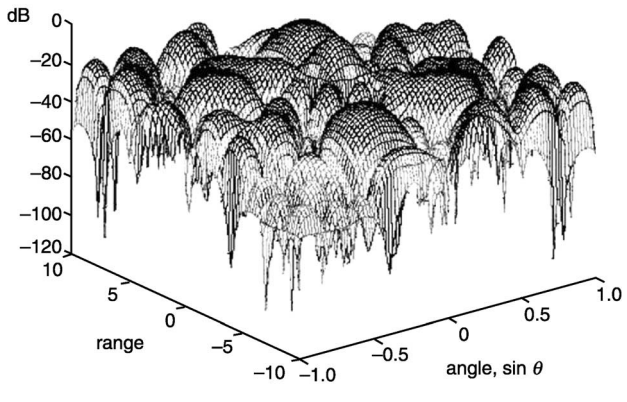

Fig. 4 *Auto-ambiguity function of Costas signal of Fig. 3 ($N = 7$)*

2.4 Summary

For this work the Costas signal is adopted for the host radar waveform because it yields a thumbtack-shaped ambiguity function with a relatively low pedestal. For a fixed number of frequency hops within a radar pulse there are many different hopping patterns that result in essentially the same thumbtack-shaped ambiguity function. Hence, different frequency-hopping patterns can be utilised to further complicate the coherent reference estimation task of the non-cooperative radar.

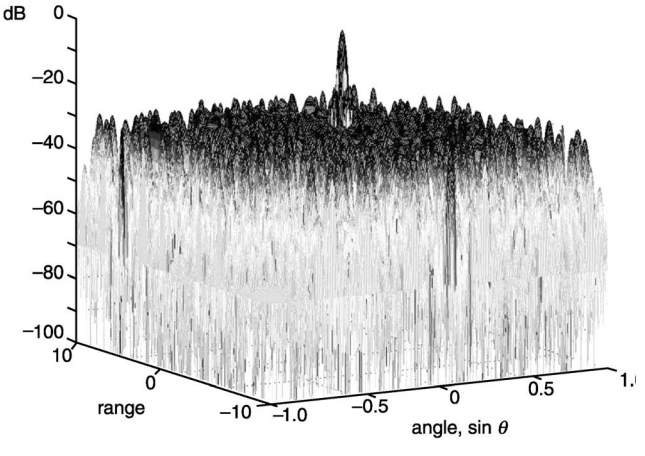

Fig. 5 *Auto-ambiguity function of Costas signal for $N = 30$*

3 Generation of radiation patterns

This Section describes two different approaches to the generation of radiation patterns for the masking signal waveform. The first of these uses an interferometer; the second is based on a Butler matrix.

3.1 Interferometer scheme

The radar antenna is assumed to be an N-element array of omnidirectional elements with interelement spacing d. The masking signal is radiated via an additional two elements, one at each end of the array (Fig. 6). The two interferometric elements are driven separately with an independent waveform generation, timing and control circuit. Ideally the interferometer antenna pattern will overlay the sidelobes of the host radar main antenna pattern with minimal overlay of the radar main beam. The interferometer may or may not be on all of the time. However, as a minimum, the interferometer will be on while the host radar is in the transmit mode with the objective that the interferometer signal will mask that portion of the host radar signal emitted through the radar sidelobes. In this way a coherent reference signal is denied to a non-cooperative bistatic receiver. To increase the effectiveness of this masking, it is also proposed to modulate the interferometer antenna pattern from pulse to pulse such that the pattern is rotated on each pulse (Fig. 7).

3.1.1 Interferometer antenna pattern: In general, the azimuthal radiation pattern of the interferometer array factor can be shown to have the following properties, with $d = \lambda/2$, $\theta = \pi/2$; α is the azimuth angle with respect to the normal to the interferometer axis:

(i) For all integer values of N (antenna array elements), either odd or even
  (a) symmetry exists about both the x- and y-axes
  (b) the number of major lobes is equal to $(2N + 2)$
  (c) there are no minor lobes
  (d) major lobes always occur at $\alpha = 0^\circ$ and 180°
(ii) When N is an odd integer
  (a) the polarity of the major lobes strictly alternate in sign from one lobe to the next
  (b) major lobes always occur at $\alpha = \pm 90^\circ$
(iii) When N is an even integer
  (a) focusing entirely above or below the x-axis, the polarity of the major lobes strictly alternate in sign from one lobe to the next
  (b) the first major lobes positioned on either side of the x-axis have the same polarity
  (c) nulls always occur at $\alpha = \pm 90^\circ$

These properties are demonstrated by the plots in Fig. 8. The nulls appearing at $\alpha = \pm 90^\circ$ when N is an even integer are of particular interest. The derivative of the array factor is zero for $\alpha = \pm 90^\circ$. Therefore the nulls at these angles have zero slope. This is consistent with the property that the first major lobes positioned on either side of the x-axis have the same polarity. This is illustrated in Fig. 9 where a cartesian plot of $F_{IFM}(\pi/2, \alpha)$, corresponding to $N = 2$, is presented with α varying from 0° to 180°. It is seen that the null at $\alpha = \pm 90^\circ$, where the polarity of $F_{IFM}(\pi/2, \alpha)$ is unchanged and the slope is zero, is noticeably broader than the nulls at $\alpha = 19.5^\circ$ and 160.5°, where the polarity of $F_{IFM}(\pi/2, \alpha)$ does change. To avoid self-jamming of the radar and communication waveforms it may be desirable to steer the interferometer pattern such that the main beam of the host radar is centred in this broad null.

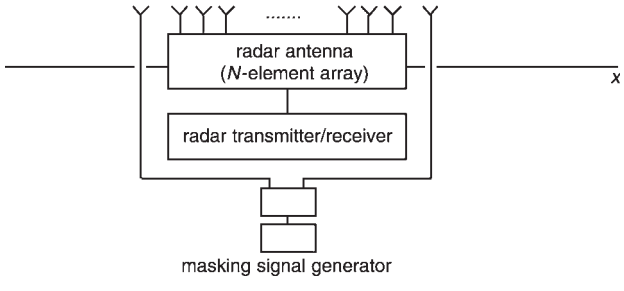

Fig. 6 *Configuration of system using interferometer*

3.1.2 Steering the interferometer: It was first assumed that the interferometer elements are placed on a linear grid about the main radar elements and the interferometer pair steered by inserting an appropriate

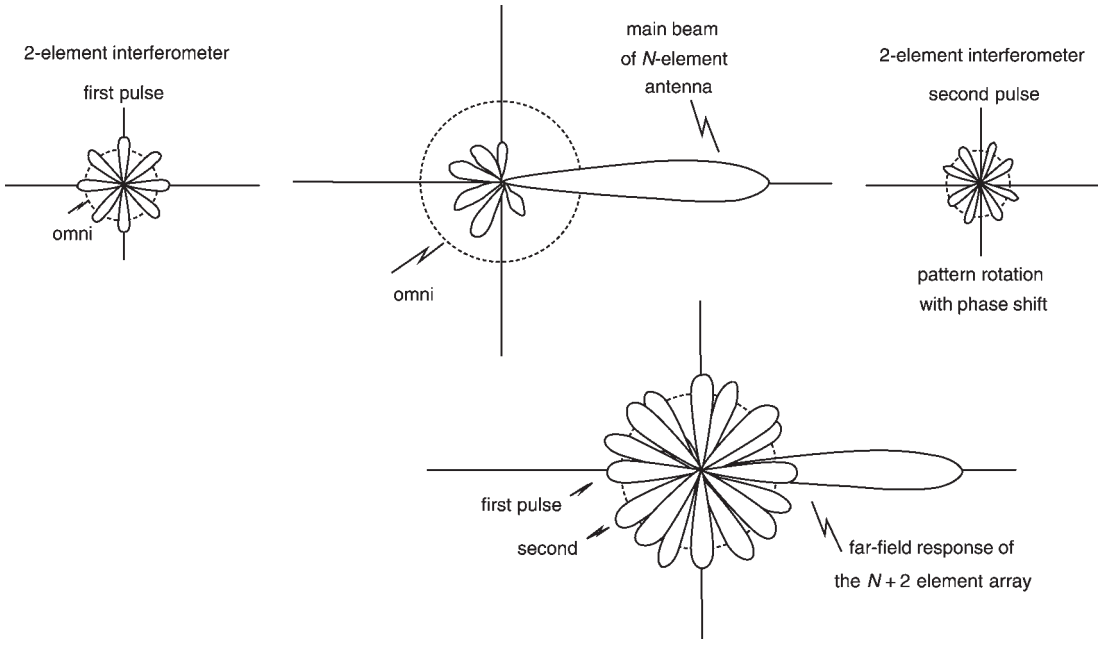

Fig. 7 *Pulse-to-pulse phase modulation of sidelobes denies coherent reference to non-cooperative receivers*

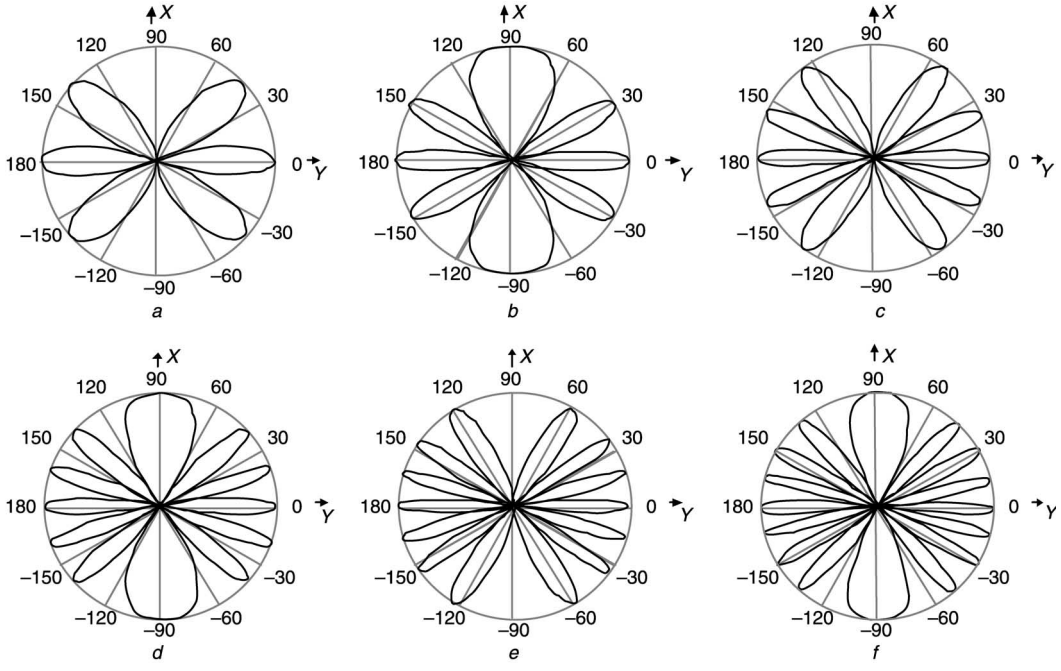

Fig. 8 *Azimuthal radiation pattern of interferometer array plotted for* $d = \lambda_0/2$, $\theta_0 = \pi/2$

a $d_{IFM} = 3\lambda_0/2$
b $d_{IFM} = 2\lambda_0$
c $d_{IFM} = 5\lambda_0/2$
d $d_{IFM} = 3\lambda_0$
e $d_{IFM} = 7\lambda_0/2$
f $d_{IFM} = 4\lambda_0$

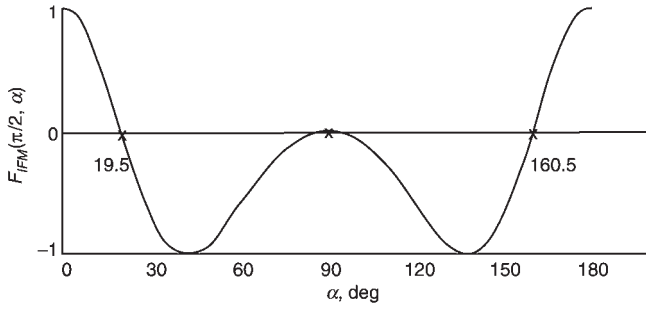

Fig. 9 *Cartesian plot of* $F_{IFM}(\pi/2, \alpha)$ *corresponding to* $N = 2$, *with* α *varying from* 0° *to* 180°

phase shift into each channel. It was noticed that severe distortion occurred in the array factor radiation pattern when the interferometer was steered and that although there was a null at $\alpha = 0^\circ$, this was not a broad null. It was concluded therefore that it is not possible to steer a broad null to $\alpha = 0^\circ$ when the interferometer is placed on a linear grid about the main radar elements.

On the other hand, a broad null was obtained at $\alpha = 0^\circ$, when the interferometer was placed on the y-axis while the linear array of the main radar remained along the x-axis. As before, the two dipole antennas of the interferometer pair were directed in the z-direction. However, the elements were now placed on the y-axis. Because the interferometer elements no longer straddle the main radar elements on the x-axis, it is convenient to measure the interferometer spacing in units of half wavelength. Therefore the interferometer spacing was defined to be

$$d_{IFM} = k_s \frac{\lambda}{2} \tag{8}$$

where k_s is an integer. Polar plots of the azimuthal radiation pattern of the interferometer array factor, where the elements are on the y-axis, are presented in Fig. 10 for $\theta = \pi/2$ and $k_s = 3, 5$, and 7. Note that these values of k_s correspond to $d_{IFM} = 3\lambda/2$, $5\lambda/2$ and $7\lambda/2$, respectively. As expected, because k_s is an odd integer for each of the plots, a broad null is seen to exist at $\alpha = 0^\circ$ in each case. Therefore, assuming that the main radar antenna elements are positioned on the x-axis while the interferometer elements are placed along the y-axis, broad nulls occur broadside to the main radar antenna in both the horizontal and vertical planes whenever k_s is an odd integer guaranteeing the orthogonality property between radar and masking signal. Since the interferometer excitation is likely to be considerably smaller than the radar excitation, placement of the broad null of the interferometer at the centre of the main beam of the radar is likely to be an effective technique for preventing the interferometer signal from interfering with the desired radar target returns.

3.2 Butler matrix scheme

Consider, as in the previous Section, an N-element linear antenna array. Suppose initially that the array is fed by a Butler matrix [15] (Fig. 11). A Butler matrix may be considered to be a hardware realisation of the Cooley–Tukey fast Fourier transform algorithm [16]. This generates a set of spatially orthogonal antenna beams, each of the form

$$|E| = \frac{1}{N} \frac{\sin(N\psi/2)}{\sin(\psi/2)} \tag{9}$$

with

$$\psi = \frac{kd}{\lambda} \sin(\theta - \delta_m) \tag{10}$$

where d is the element spacing, λ is the wavelength, $k = 2\pi/\lambda$, θ is the azimuth angle and δ_m is the angle of the maximum of the mth beam. For an N-element array

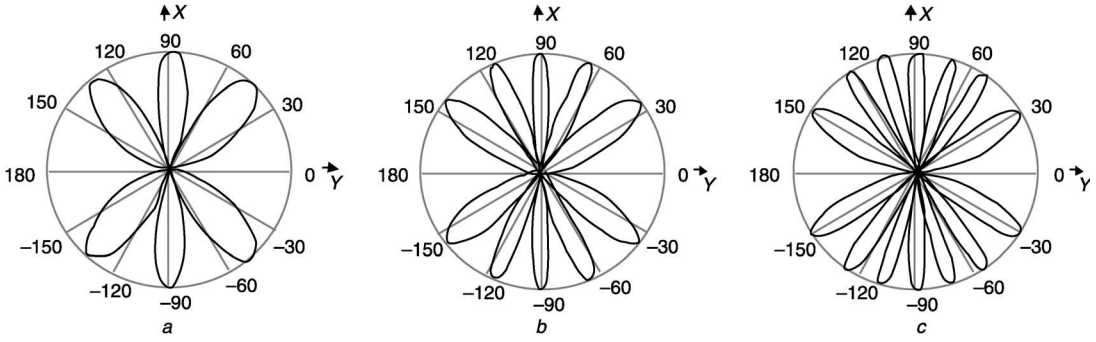

Fig. 10 *Azimuthal radiation pattern of interferometer array factor, where elements are on the y-axis, for* $\theta_0 = \pi/2$
a $d_{IFM} = 3\lambda_0/2$
b $d_{IFM} = 5\lambda_0/2$
c $d_{IFM} = 7\lambda_0/2$

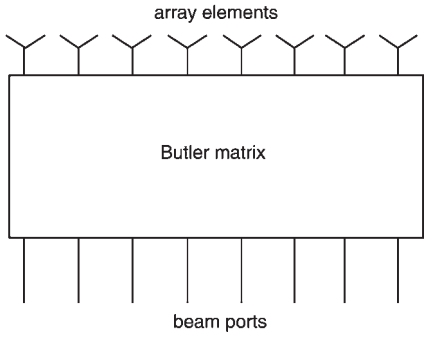

Fig. 11 *Configuration of system using Butler matrix in which the beam ports provide set of orthogonal beams*
One beam is used for the radar, and the masking signal radiated, at a suitable power level, from the others

$$\delta_m = \frac{(2m-1)\pi}{N} \tag{11}$$

so the normalised far-field pattern of the mth beam is

$$E_m = \frac{1}{N}\frac{\sin\left[\frac{N\pi d}{\lambda^2}\sin\left(\theta - \frac{(2m-1)\pi}{N}\right)\right]}{\sin\left[\frac{\pi d}{\lambda^2}\sin\left(\theta - \frac{(2m-1)\pi}{N}\right)\right]} \tag{12}$$

The orthogonality of this set of beams is maintained over a broad bandwidth, dictated by the hardware of the Butler matrix but typically an octave or more. For this to be so, the beamwidths and directions of the beams must change with frequency. The beams have a first sidelobe level of -13.2 dB, which is rather high for radar purposes; the sidelobe level can be lowered by an amplitude taper across the array in the usual way, but this destroys the orthogonality condition. The set of beams may be steered electronically by a set of phase shifters at the antenna elements.

Suppose that one of the central beams is used for the radar, both for transmitting and receiving. One or more of the remaining beams is used to radiate the masking signal or signals, at an appropriate relative power level.

Furthermore, if the radar signal and masking signals were to be generated at the beam ports of the Butler matrix by direct digital synthesis, which could include the effect of phase shifts to steer the beams electronically, then since the signals radiated from each element are simply weighted combinations of the beam port signals, the element signals may be calculated and generated directly without any need for the Butler matrix hardware.

4 Results

To assess whether the level of masking is sufficient to mask the radar signal to an adversary, and hence to deny a reference for bistatic operation, a radar signal to masking signal ratio for the case of an adversary listening from a particular angle θ is defined:

$$L(\theta) = \frac{\text{level of masking signal}}{\text{level of radar signal}} \tag{13}$$

This can be evaluated either at a particular value of θ, or as an average over the sidelobe region. The value of L at $\theta = 0$ (i.e. at the centre of the host radar main lobe) will obviously take negligible values first because of the broad null of the masking signal at this angle and secondly because of the orthogonal coding of the signals. An adversary could only recover the radar signal if listening from that specific direction.

The further the angle of the adversary from boresight $(\theta = 0)$, the worse the recovery. This is because we can vary the radar to masking signal ratio by varying the power of the transmitted masking signal in order to cause considerable disruption of the reception of the radar signal while of course maintaining consistent radar operation.

We wish to quantify the degree of masking of the radar signal at a receiver in a given direction, and the degree of suppression of echoes (from targets or from clutter) of the masking signal received in the channels of the radar receiver. To achieve this we formulated a radar-to-masking signal ratio and a radar signal echo to masking signal echo ratio explained in the following Sections.

4.1 Radar signal to masking signal ratio

Following (13) in the previous Section the radar signal to masking signal as a function of angle will be

$$L(\theta) = \frac{P_r F_r(\theta)}{P_m F_m(\theta)} \tag{14}$$

This ratio depends on the geometry of the antennas used and their radiation patterns. In the following Section we investigate how this ratio is expressed for the interferometer and Butler matrix cases.

4.1.1 Interferometer: The main radar array factor is given by

$$F_r(\theta, \alpha) = \frac{1}{\lambda}\frac{\pi d \sin\theta \sin\alpha}{\sin\left(\frac{\pi d}{\lambda}\sin\theta \sin\alpha\right)} \tag{15}$$

The masking signal array factor when the interferometer scheme is used is given by

$$F_m(\theta,\alpha) = \cos\left(\pi \frac{d_{IFM}}{\lambda} \sin\,\theta \cos\,\alpha\right) \tag{16}$$

So the radar signal to masking signal ratio when an interferometer is used would be

$$L(\theta)_{IFM} = \frac{P_r F_r(\theta)}{P_m F_m(\theta)} = \frac{P_r}{P_m} \frac{\pi d \sin\,\theta \sin\,\alpha}{\lambda \sin\left(\frac{\pi d}{\lambda} \sin\,\theta \sin\,\alpha\right) \cos\left(\pi \frac{d_{IFM}}{\lambda} \sin\theta \cos\,\alpha\right)} \tag{17}$$

4.1.2 Butler matrix: As in the previous Section, the main radar array factor is given by

$$F_r(\theta,\alpha) = \frac{1}{\lambda} \frac{\pi d \sin\,\theta \sin\,\alpha}{\sin\left(\frac{\pi d}{\lambda} \sin\,\theta \sin\,\alpha\right)}$$

The masking signal array factor for the Butler matrix scheme is given by

$$F_m(\theta,\alpha) = \frac{1}{\lambda} \frac{\pi d \sin(\theta-\delta) \sin\,\alpha}{\sin\left(\frac{\pi d}{\lambda} \sin(\theta-\delta) \sin\,\alpha\right)} \tag{18}$$

The radar signal to masking signal ratio for the Butler matrix scheme is therefore

$$L(\theta)_{BM} = \frac{P_r}{P_m} \cdot \frac{\sin\,\theta \sin\left(\frac{\pi d}{\lambda} \sin(\theta-\delta) \sin\,\alpha\right)}{\sin(\theta-\delta) \sin\left(\frac{\pi d}{\lambda} \sin\,\theta \sin\,\alpha\right)} \tag{19}$$

It is evident that in a given direction θ, the ratio $F_m(\theta)/F_r(\theta)$ will be constant. Therefore the power levels P_m, P_r are the only parameters that need to be adjusted to achieve a desired degree of masking.

4.2 Suppression of masking signal in radar receiver

The suppression of the masking signal in the radar receiver will include the echoes received from the target and clutter. The masking signal levels will be further suppressed because the filter at the receiver is matched to the radar signal.

The echo of the masking signal is proportional to $P_m F_m$. Similarly the echo of the radar signal is proportional to $P_r F_r$. These signals are received by the radar antenna pattern which we will consider to be the same as the transmit radar pattern. The following two expressions can thus be written:

$$S_m = P_m F_m(\theta_{TAR}) F_r(\theta_{REC}) \tag{20}$$

$$S_r = P_r F_r(\theta_{TAR}) F_r(\theta_{REC}) \tag{21}$$

These are applied to the matched filter for the radar signal. The degree of suppression of the masking signal is therefore

$$R(\theta) = \frac{P_m F_m(\theta_{TAR}) F_r(\theta_{REC}) \int_{-\infty}^{\infty} u_m(t-\tau) u_r^*(t) e^{j2\pi f_D t}\,dt}{P_r F_r(\theta_{TAR}) F_r(\theta_{REC}) \int_{-\infty}^{\infty} u_r(t-\tau) u_r^*(t) e^{j2\pi f_D t}\,dt} \tag{22}$$

where $F_m(\theta_{TAR})$ is the Doppler shifted echo of the masking signal from the target; $F_r(\theta_{TAR})$ is the Doppler shifted echo of the radar signal from the target; $F_r(\theta_{REC})$ is the radar signal at reception;

$$\int_{-\infty}^{\infty} u_m(t-\tau) u_r^*(t) e^{j2\pi f_D t}\,dt$$

is the response to the masking signal of the filter matched to the radar signal (cross-ambiguity function); and

$$\int_{-\infty}^{\infty} u_r(t-\tau) u_r^*(t) e^{j2\pi f_D t}\,dt$$

is the response to the radar signal of the filter matched to the radar signal (auto-ambiguity function).

As a result it can be seen that the radar signal echo to masking signal echo ratio depends on the relative transmitted levels of the radar signal and masking signal, as well as the responses of the radar and masking signals at a given Doppler shift to the filter matched to the radar signal at zero Doppler. All of this also depends on the position of the target, so it is not controllable by the radar designer. However, the power levels P_m and P_r of the radar and masking signals are controllable and can be set to achieve the desired results.

As examples, Figs. 12 and 13 show the degree of suppression of the masking signal in the radar receiver, calculated according to (22), for the cases of the interferometer scheme and the Butler matrix scheme,

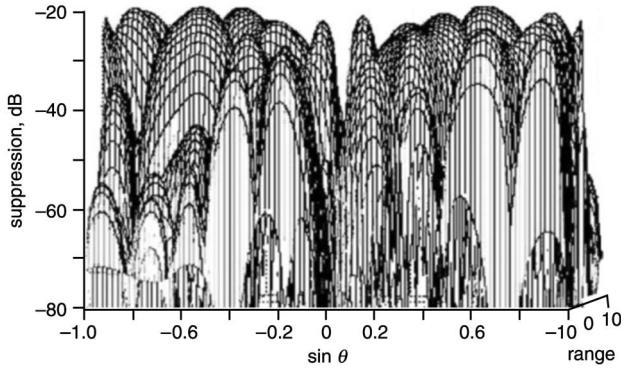

Fig. 12 *Degree of suppression of masking signal in radar receiver (for Costas signal of Figs. 3 and 4 and $P_r/P_m = 20$ dB), interferometer case*

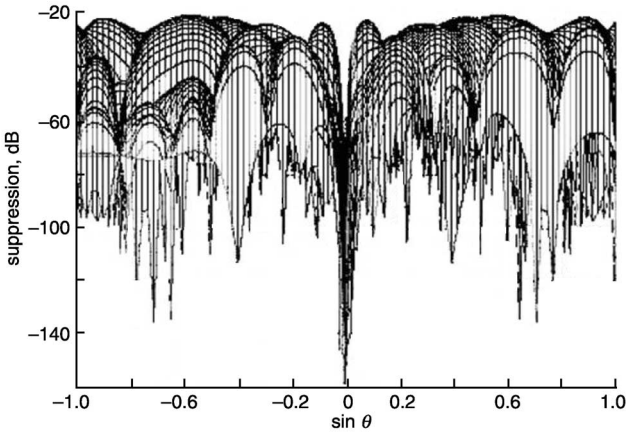

Fig. 13 *Degree of suppression of masking signal in radar receiver (for Costas signal of Figs. 3 and 4 and $P_r/P_m = 20$ dB), Butler matrix case*

Side-on view shows shape of null at $\theta = 0$, both because of low level of jamming signal radiated around that direction and because code orthogonality is good close to zero Doppler

respectively. For both plots the ratio of masking signal to radar signal P_r/P_m has been chosen to be 20 dB, which gives an acceptable degree of masking in the sidelobe region. In both Figures it can be seen that close to zero Doppler the rejection of the masking signal in the radar receiver is almost total, both because of the level of the jamming signal radiated around that direction and because the code orthogonality is good close to zero Doppler. Away from this direction the rejection degrades, to a minimum value of about 30 dB in each case, corresponding to an average value of about 35 dB.

5 Conclusions

5.1 Summary

We have introduced and analysed a set of theoretical techniques to prevent a radar being used by a bistatic receiver as a non-cooperative illuminator by radiating in addition to the radar signal waveform a 'masking signal' waveform. This is designed to be orthogonal to the radar signal waveform, both in the coding domain and the spatial domain. A number of waveform coding techniques have been analysed, and of those considered, Costas codes appear to offer best performance and flexibility. Two spatial coding techniques have been devised and analysed; one based on an interferometer, and one based on a Butler matrix. Expressions as a function of the system parameters have been derived for the degree of suppression of the radar signal by the masking signal, and for the suppression of the masking signal in the host radar echo. Evaluation and plotting of these expressions have demonstrated that it is possible to obtain adequate masking of the radar signal, while at the same time achieving suppression of echoes from the masking signal of the order of 30 or 40 dB. In this respect the performance of the interferometer and Butler matrix schemes are comparable.

5.2 Further work

Both interferometer and Butler matrix schemes appear to give acceptable results, and both are worthy of further investigation. The Costas codes used in the examples presented in Figs. 12 and 13 are of length 7, and improved performance could probably be obtained by using longer Costas codes, or orthogonal codes of other kinds. For the Butler matrix scheme it would be interesting to examine the tradeoff between sidelobe level and beam orthogonality. Also, in the treatment so far it has been assumed that the radar signal radiation patterns are identical on transmit and on receive. It would be interesting to explore the use of non-identical antenna patterns, and indeed it may be anticipated that the use of STAP-type methods to adaptively suppress clutter returns from the masking signal would give good results. Finally, the hardware implications of using direct digital synthesis, for example in the requirement for power amplifiers with very low intermodulation, should be looked at critically.

The ideas presented are just one example of the idea of 'waveform diversity', in which waveform coding techniques are used with multiple transmit and receive beams, probably in conjunction with adaptive processing in spatial and temporal domains. Central to the analysis of such schemes is the cross-ambiguity function, weighted by the appropriate transmit and receive radiation patterns It should be possible to generalise the formulation to other types of system, to situations where the transmit and receive antenna patterns are different, and to broadband signals.

It may also be interesting to investigate whether it is possible to design the spatial denial signal to carry useful information, such as air-to-ground telemetry or navigation signals, as well as the bistatic masking function. This imposes an additional constraint, but it may be possible also to design the radar waveform signal adaptively in real time, so as to maintain the coding orthogonality.

6 Acknowledgments

This work has been supported by the US Air Force Office of Scientific Research (Dr. John Sjogren) and by AFRL/SNRT (Gerard Genello). The authors express their thanks to Dr. Richard Schneible and Kenneth Stiefvater, of Steifvater Consultants, for invaluable discussions.

7 References

1 Willis, N.J.: 'Bistatic radar' (Artech House, Boston, 1991)
2 Dunsmore, M.R.B.: 'Bistatic radars', in Galati, G. (Ed.): 'Advanced radar techniques and systems' (Peter Peregrinus, Stevenage, 1993), Chap. 11
3 Griffiths, H.D., and Carter, S.M.: 'Provision of moving target indication in an independent bistatic radar receiver', *Radio Electron. Eng.*, 1984, **54**, (7/8), pp. 336–342
4 Thomas, D., Jr.: 'Synchronization of non-cooperative bistatic radar receivers'. PhD dissertation, Syracuse University, NY, 1999
5 Wicks, M.C., Bolen, S.M., and Brown, R.D.: 'Waveform diversity for spatial–temporal denial of radar and communications systems'. US patent 6,204,797, 20 March 2001
6 Ertan, S., Wicks, M.C., Antonik, P., Adve, R., Weiner, D., Griffiths, H.D., and Fotinopoulos, I.: 'Bistatic denial by spatial waveform diversity'. Proc. IEE Conf. Radar 2002, Edinburgh, UK, 15–17 Oct. 2002, IEE Conf. Publ. 490, pp. 17–21
7 Woodward, P.M.: 'Probability and information theory, with applications to radar' (Pergamon Press, London, 1953; republished by Artech House, Dedham MA, 1980)
8 Rihaczek, A.W.: 'Principles of high resolution radar' (McGraw-Hill, New York, 1969; republished by Artech House, Norwood, MA, 1996)
9 Giuli, D., Fossi, M., and Facheris, L.: 'Radar target scattering matrix measurement through orthogonal signals', *IEE Proc. F, Radar Signal Process.*, 1993, **140**, (4), pp. 233–242
10 Griffiths, H.D., and Normant, E.: 'Adaptive SAR beamforming network'. European Space Agency Contract Report, Contract 6553/89/NL/IW, 1990, ESA Technical and Publications Branch, ESTEC, Noordwijk
11 Levanon, N.: 'Radar principles' (Wiley, New York, USA, 1988)
12 Nathanson, F.E.: 'Radar design principles' (McGraw-Hill, New York, 1991, 2nd edn.)
13 Golomb, S.W., and Taylor, H.: 'Construction and properties of Costas arrays', *Proc. IEEE*, 1984, **72**, (9), pp. 1143–1163
14 Costas, J.P.: 'A study of a class of detection waveforms having nearly ideal range-Doppler ambiguity properties', *Proc. IEEE*, 1984, **72**, pp. 996–1009
15 Butler, J.L.: 'Digital, matrix and intermediate-frequency scanning', in Hansen, R.C. (Ed.): 'Microwave scanning antennas', Vol. 3 (Peninsula Publishing, 1985)
16 Cooley, J.W., and Tukey, J.W.: 'An algorithm for the machine calculation of a complex Fourier series', *Math. Comput.*, 1965, **19**, pp. 297–301